SCIENTIFIC REPORTS

OPEN

SUBJECT AREAS:
SYNTHESIS AND PROCESSING
INFORMATION STORAGE
CHARACTERIZATION AND ANALYTICAL TECHNIQUES
SURFACES, INTERFACES AND THIN FILMS

Received
29 September 2014

Accepted
4 December 2014

Published
14 January 2015

Correspondence and requests for materials should be addressed to C.S.B. (elebcs@nus.edu.sg)

Understanding the Role of Nitrogen in Plasma-Assisted Surface Modification of Magnetic Recording Media with and without Ultrathin Carbon Overcoats

Neeraj Dwivedi[1], Reuben J. Yeo[1], Nalam Satyanarayana[1], Shreya Kundu[1], S. Tripathy[2] & C. S. Bhatia[1]

[1]Department of Electrical and Computer Engineering, National University of Singapore, Singapore 117583, [2]Institute of Materials Research and Engineering (IMRE), A*STAR (Agency for Science, Technology, and Research), 3 Research Link, Singapore 117602.

A novel scheme of pre-surface modification of media using mixed argon-nitrogen plasma is proposed to improve the protection performance of 1.5 nm carbon overcoats (COC) on media produced by a facile pulsed DC sputtering technique. We observe stable and lower friction, higher wear resistance, higher oxidation resistance, and lower surface polarity for the media sample modified in 70%Ar + 30%N_2 plasma and possessing 1.5 nm COC as compared to samples prepared using gaseous compositions of 100%Ar and 50%Ar + 50%N_2 with 1.5 nm COC. Raman and X-ray photoelectron spectroscopy results suggest that the surface modification process does not affect the microstructure of the grown COC. Instead, the improved tribological, corrosion-resistant and oxidation-resistant characteristics after 70%Ar + 30%N_2 plasma-assisted modification can be attributed to, firstly, the enrichment in surface and interfacial bonding, leading to interfacial strength, and secondly, more effective removal of ambient oxygen from the media surface, leading to stronger adhesion of the COC with media, reduction of media corrosion and oxidation, and surface polarity. Moreover, the tribological, corrosion and surface properties of mixed Ar + N_2 plasma treated media with 1.5 nm COCs are found to be comparable or better than ~2.7 nm thick conventional COC in commercial media.

Areal densities of hard disk drives (HDDs) have been growing at an incredible pace, and are expected to approach 1 terabit per square inch (Tb/in^2) by 2014[1]. Currently, the goal of the HDD industry is to advance the areal density beyond 1 Tb/in^2. This requires significant improvement in all aspects of the HDD system[2–6]. Reducing the head-media spacing (HMS) is a crucial approach to achieve increased areal densities for future HDDs. To protect the hard disk media from corrosion and mechanical wear, and hence enhance the durability of HDDs, the media is coated with a thin carbon overcoat (COC) and a very thin lubricant layer. Since the COC is the main contributor of the HMS, its thickness must be reduced significantly to achieve a high areal density. Based on industry roadmaps, the average HMS and COC thickness should be reduced to ~5 nm and ~1.6 nm, respectively[1], to achieve an areal density of 4 Tb/in^2.

For a long time, magnetron sputtering has been the chosen deposition process for ultrathin COCs on media[7–9]. However, sputtered COCs are unable to provide adequate protection for the media when they are thinned down to 2–3 nm or less[10,11]. Presently, plasma enhanced chemical vapor deposition (PECVD) is used to deposit 2.5–3 nm thin hydrogenated carbon (CH_x) overcoats[1,12]. However, when the thickness is reduced to below 2 nm, the protective characteristics of CH_x-based COCs also start to deteriorate. Moreover, CH_x-based overcoats have shown poor thermal stability in heat-assisted magnetic recording (HAMR) conditions, which would be used in HDDs in the near future[13–15]. Another deposition technique known as filtered cathodic vacuum arc (FCVA) has demonstrated the capability to produce ultrathin COCs with enhanced protection characteristics at thicknesses less than 2 nm[16–20]. Moreover, FCVA-deposited COCs have shown excellent thermal stability to be used for HAMR[13,14,21]. However, particle generation remains an issue with FCVA-deposited COCs, which may lead to slider and media wear along with flyability issues[17,19,22]. Since magnetron sputtering is a simple, inexpensive and industrial-friendly process for the deposition of overcoats with negligible particle generation, the industry and researchers are still using this process for the fabrication of carbide and non-carbon-based overcoats[23–26]. For example, recently Rose *et al.*[25,26] have fabricated a variety of carbide and non-carbide overcoats such as SiN, SiC,

TiSiN, TiSiC by magnetron sputtering. They found that TiSiC and TiSiN overcoats provide significant protection against corrosion, mainly in the case of TiSiC and TiSiN overcoats at thickness of ~2.5 nm. Although the good corrosion barrier characteristic of TiSiN and TiSiC is interesting, the structures of these overcoats are complex due to their three-element composition, making it difficult to maintain the stoichiometry. Nevertheless, this has motivated researchers to explore magnetron sputtering for new and simpler overcoat designs/materials or approaches to improve the characteristics of existing COCs and other overcoats. In this context, improving the protection characteristics of ultrathin sputtered COCs of thickness <2 nm by a novel approach such as a pre-overcoat media surface modification process would be of significant interest.

Surface nitriding is well-known to be an effective approach to improve the resistance of engineering materials to wear and corrosion. One of the industrial techniques applied in surface nitriding is exposing the material (usually a metal or its alloy) to nitrogen gas at elevated temperatures (~800°C), to allow the nitrogen to diffuse into the metal surface[27]. On the other hand, plasma-assisted nitriding is another popular industrial process which requires relatively lower temperatures (between 260 to 500°C) and shorter treatment times, due to the ionization of nitrogen in the plasma[28]. Hence, nitrogen-based surface modification of hard disk media is perhaps one of the ways to improve its wear and corrosion resistance, but it needs an appropriate selection of the process and its parameters for the treatment. Since the usual nitriding process takes place at very high temperatures for long durations of time, this process cannot be suitable for surface treatment of hard disk media as it may damage the magnetics of the media. Nevertheless, nitrogen plasma-assisted treatments can be used for surface modification of media but the treatment parameters such as process temperature and process time must be very low with good control over the process. It should be noted that this approach of nitrogen plasma-assisted treatment of magnetic media followed by deposition of an ultrathin COC has not yet been explored for magnetic storage application.

In this work, we employ a novel surface modification technique where the media surface is subjected to mixed argon-nitrogen plasma at room temperature for a very short time, with the aim of tailoring the surface and interface properties for enhanced wear and corrosion protection. Three different gaseous compositions of Ar and Ar + N_2 are used to generate the plasmas for each surface modification process to investigate and optimize the Ar + N_2 mixture for the best performance. We call this process nitrogen plasma-assisted surface modification of media, because unlike plasma-assisted nitriding, it is performed at much shorter times (3 min only) and at room temperatures (much lower temperatures). For each gaseous composition, two types of samples were prepared: 1) surface modified media without a COC; and 2) surface modified media with an ultrathin 1.5 nm COC. The samples were then tested and characterized in terms of their tribological, surface, electrochemical corrosion, oxidation and magnetic properties, as well as their microstructures.

Results

Figure 1 schematically demonstrates the Ar and mixed Ar + N_2 plasma-assisted surface modification of bare magnetic media, and the deposition of COC on surface modified media for the preparation of different samples used in this work. CoCrPt:oxide-based bare magnetic media (BMM) were used as the starting substrates (Figure 1a), which were then exposed to Ar/Ar + N_2 plasma in the sputtering chamber for surface modification (Figure 1b). This led to the preparation of the first series of surface modified media samples without COCs (Figure 1c) as: samples S-1 (surface modification using 100%Ar plasma), S-2 (surface modification using mixed 70%Ar + 30%N_2 plasma) and S-3 (surface modification using mixed 50%Ar + 50%N_2 plasma). The deposition of ultrathin COCs was done on surface modified media using the pulsed DC (PDC) sputtering process (Figure 1d). Thus, the second series of surface modified media samples with COCs (Figure 1e) are: sample S-4 (surface modification using 100%Ar plasma + 1.5 nm COC), sample S-5 (surface modification using mixed 70%Ar + 30%N_2 plasma + 1.5 nm COC) and sample S-6 (surface modification using mixed 50%Ar + 50%N_2 plasma + 1.5 nm COC). Apart from these samples, we have also included current commercial media with commercial COC of thickness ~2.7 nm as a reference sample (S-7) to compare the functional performance of our samples and commercial media (See *supplementary information S1* for a table which summarizes the description of all the samples used in this work). In view of different plasma conditions, the etched thickness for each plasma condition was also determined (*See supplementary information S2*).

Thickness and surface roughness. After the samples preparation, the thickness of COCs in different samples was measured using cross-section high resolution transmission electron microscopy (HRTEM, *see supplementary information S3*). The thicknesses of the COCs in samples S-4 to S-6 were each measured to be 1.5 ± 0.1 nm, while the thickness of COC in sample S-7 was measured to be 2.7 ± 0.1 nm.

The average roughness (R_a) and root-mean-square roughness (R_q) of all the samples were measured by tapping mode atomic force microscopy (AFM) (*see supplementary information S4*). The values of R_a in all the samples were found to be slightly lower than the values of R_q. Interestingly, the disks, which were subjected to the surface modification process using only Ar plasma (100%Ar, sample S-1), showed slightly but significantly higher surface roughness than the disks modified using plasma with gaseous mixtures of Ar + N_2 (samples S-2 and S-3). This indicates that the inclusion of nitrogen in mixed Ar + N_2 plasma could have assisted in smoothening the surface of the media. Nevertheless, no significant difference in the surface roughness was observed between samples S-2 and S-3. Similarly, when pulsed DC sputtered COCs were applied onto either 100%Ar plasma or mixed Ar + N_2 plasma modified disks, the surface roughness of the media was found to be almost similar with an R_q value consistently <0.2 nm (~0.15 nm). Such low values of R_q have been reported for sputtered ultrathin nitrogenated carbon (CN_x) films, but they were deposited onto silicon substrates[29]. In our case, the observation of such low roughness values for sputtered COCs on hard disk media is very interesting. On the other hand, the R_q of commercial COC in sample S-7 was found to be ~0.3 nm, which was nearly double compared to the other samples. Minimizing the surface roughness is desirable not only for reducing HMS, but also for contributing to better flyability and good tribological and corrosion properties. Hence, using a gaseous mixture of Ar + N_2, plasma-assisted surface modification seems to be a simple and effective way to reduce the surface roughness of hard disk media.

Tribological properties. The tribological properties of these samples were compared based on: 1) the condition of the worn surfaces of the sample and counterface ball, and 2) their frictional curves, where the coefficient of friction (COF) is plotted against the number of wear cycles (wear duration). The comparisons of frictional curves of plasma-assisted surface modified media samples without COCs and with COCs are shown in Figures 2a and 2b, respectively, and optical images of the counterface ball and wear track regions are depicted in Figure 2c. We first discuss the role of the composition of gases in plasma-assisted surface modification of media without COCs. It is evident from Figure 2a that the media modified with 100%Ar plasma (sample S-1) demonstrated the highest COF of ~0.7–0.8 until the completion of the test. There was also a considerably large amount of wear debris transferred to the ball and a severe wear track on the sample. However, when the media was subjected to the plasma with gaseous composition of 70%Ar + 30%N_2 during surface modification (sample S-2), the value of COF was found to be significantly lower (~0.3 and less) in the first 3,000

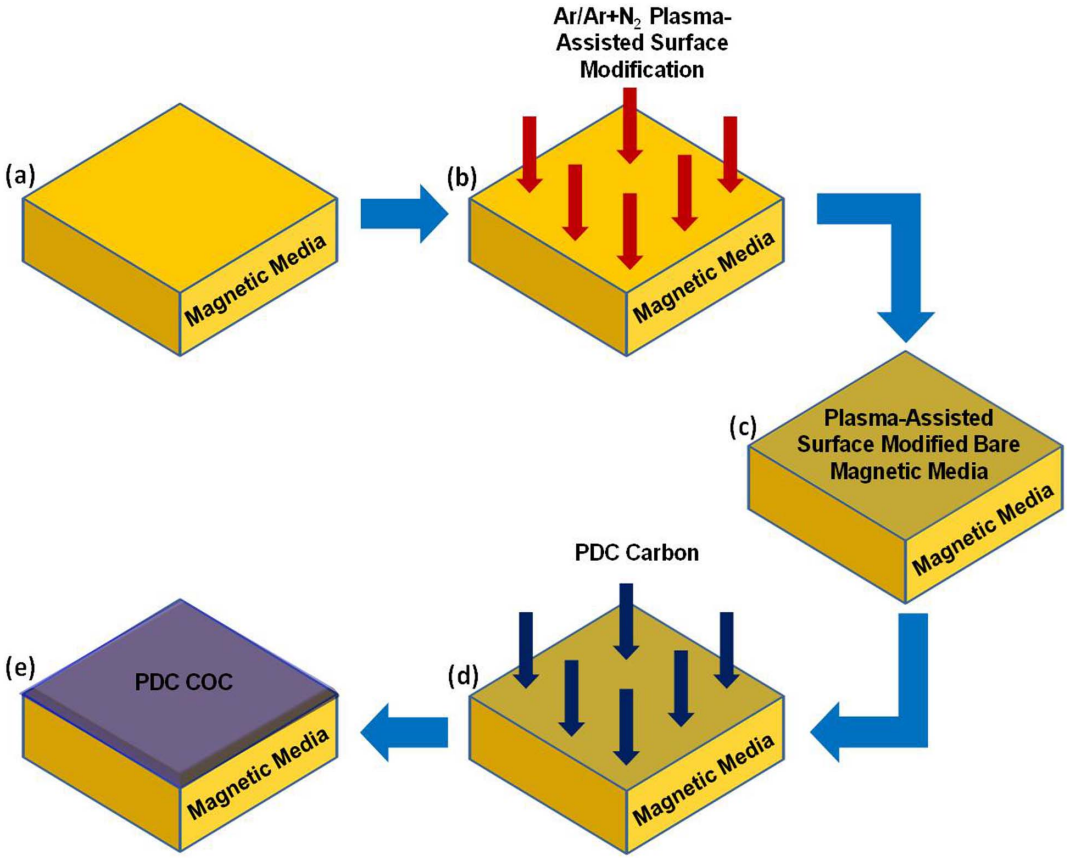

Figure 1 | Schematic representation of the substrate and deposition process. The starting substrates were (a) CoCrPt:oxide-based bare magnetic media, (b) Ar/Ar + N_2 plasma-assisted surface modification of the media, (c) surface modified bare magnetic media, (d) deposition of ~1.5 nm COC on the surface modified media using pulsed DC sputtering, and (e) surface modified media after COC deposition. The Ar/Ar + N_2 plasma-assisted surface modification of the media was performed using gaseous compositions of 100%Ar, 70%Ar + 30%N_2 and 50%Ar + 50%N_2.

cycles, after which it increased between 3,000 and 6,000 cycles, and finally saturated at a value of ~0.65 beyond 6,000 cycles. Moreover, sample S-2 showed less wear debris transferred to the ball and a less severe wear track on the sample, when compared with sample S-1. This clearly highlights the effect of introducing 30%N_2 in the mixed Ar + N_2 plasma, which helps to reduce the COF and improve the wear resistance of the media after surface modification. However, when the amount of N_2 was increased to 50% (sample S-3), the value of COF approached a value similar to that of sample S-1, although material transfer to the ball and wear track was less than that in sample S-1. Based on the above results, it was observed that 30%N_2 in mixed Ar + N_2 plasma is the best amount which improves the tribological properties of the media.

When COCs were applied on the surface modified media, the value of COF was significantly reduced and the wear resistance was considerably improved, when compared with media without COCs. However, while examining the tribological properties of surface modified media with COCs where the COCs thicknesses were kept constant in all the samples, the role of the gaseous composition during the plasma-assisted media surface modification process was clearly visible. Among samples S-4, S-5 and S-6, the best tribological performance was observed in sample S-5, giving a stable and low COF (~0.25), negligible wear debris on the ball, and no visible wear track. This suggests that the inclusion of 30%N_2 in mixed Ar + N_2 plasma has an advantageous effect in improving the tribological properties and wear resistance of the media with ~1.5 nm COC. Similarly, while comparing the tribological properties of samples S-4 with S-6, sample S-6 showed comparatively better tribological performance in terms of lower COF and higher wear resistance with the introduction of 50%N_2 during media surface modification. What is remarkable is that sample S-5, which contains only ~1.5 nm COC by simple pulsed DC sputtering after plasma-assisted surface modification of media in 70%Ar + 30%N_2, exhibited a stable and lower COF as well as higher wear resistance than current commercial media containing a significantly thicker commercial COC of ~2.7 nm (sample S-7). Sample S-7 showed COF values fluctuating between 0.3–0.4 as well as significant material transfer to the ball and a visible wear track in the worn area of the sample. The tribological properties of current commercial media with ~2.7 nm COC and ~1 nm lubricant were also investigated, and the results showed comparable or even slightly higher COF, larger material transfer to the ball, and visible wear track in this sample as compared to sample S-7 (results are not included in this manuscript). These results revealed that prior surface modification of media using a gaseous Ar + N_2 mixture (especially a composition of 70%Ar + 30% N_2) before simple pulsed DC sputtering of COC could be a facile and effective technique to achieve low friction and high wear resistance protective overcoats on media. To check the consistency of the results, the tribological tests were repeated on three different locations per sample as well as on more than one sample. The results were found to be similar.

It is important to mention that the etched thickness with 70%Ar + 30%N_2 plasma was slightly higher than the samples treated using 50%Ar + 50%N_2 plasma for constant 3 min etch time. So, two additional samples were fabricated using 50%Ar + 50%N_2 plasma – one without COC (sample S-8) and one with 1.5 nm COC (sample S-9), for a longer time to obtain the similar etch thickness as obtained using 70%Ar + 30%N_2 plasma. Tribological and roughness measurements were also conducted on these newly prepared samples (*See supplementary information S5*). We did not see improvement in the roughness and tribological properties in samples S-8 and S-9 as

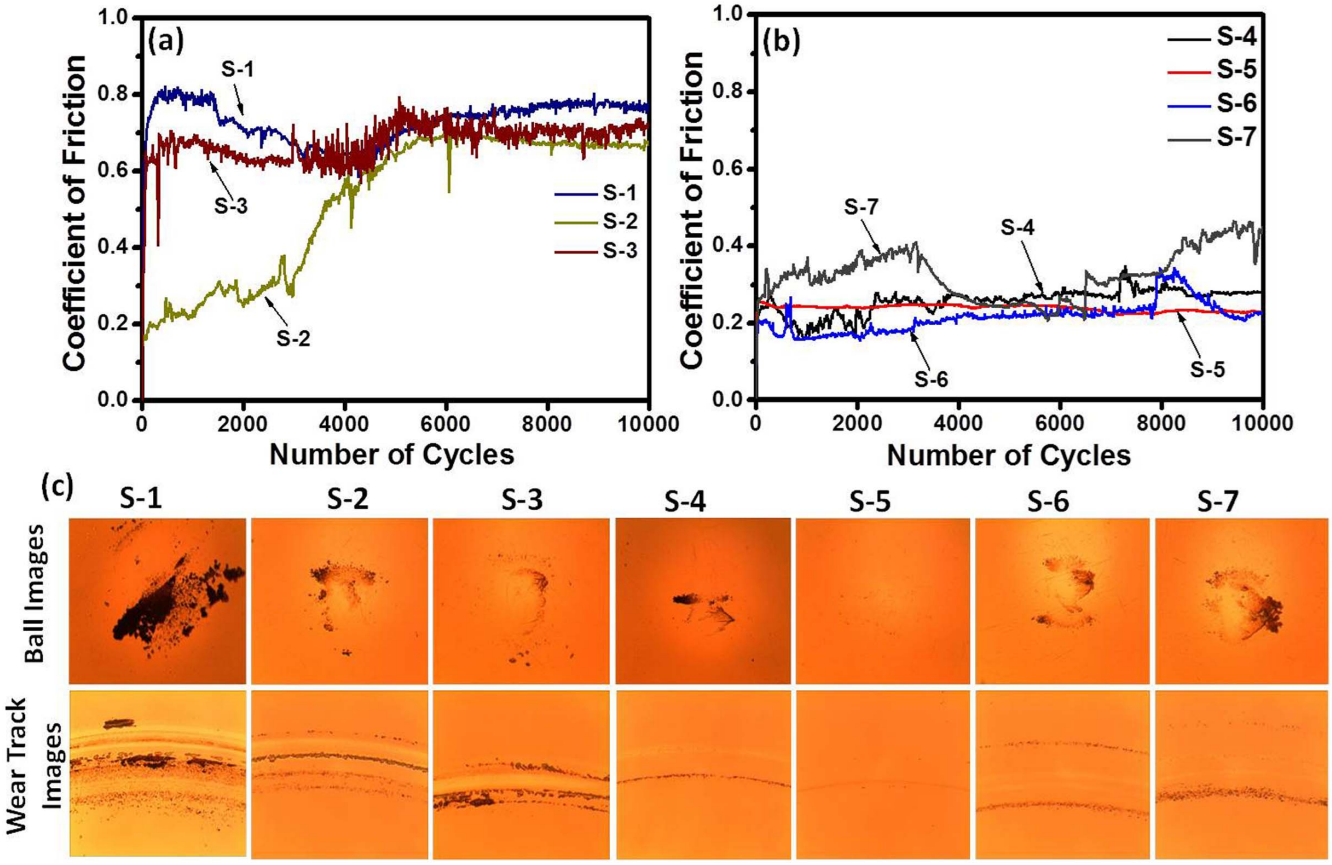

Figure 2 | Tribological properties. (a) Frictional results of surface modified media without COCs, (b) frictional results of surface modified media with ~1.5 nm COCs and commercial media with 2.7 nm COC, and (c) optical microscopic images of the ball and wear tracks for all samples after ball-on-disk tribological tests.

compared to samples S-3 and S-6 (they even showed slightly poorer properties). Hence, we concentrate on samples S-1 to S-7 for this study, out of which the constant 3 min plasma treatment time was used for the preparation of samples S-1 to S-6.

Electrochemical corrosion and surface energy. One of the purposes for employing the combination of plasma-assisted surface modified media with COCs is to improve the corrosion protection of underlying media even with the COC thickness of <2 nm. The corrosion behavior of these samples was compared based on the corrosion current density (j_{corr}), which was measured by the *Tafel* extrapolation method[30]. The j_{corr} is a measure of corrosion in the sample and varies inversely with corrosion resistance, i.e. the higher the j_{corr} value, the lower is the corrosion resistance of the sample. Figure 3a shows the variation of j_{corr} for different samples. It is evident from Figure 3a that 100%Ar plasma-assisted surface modified bare media without COC (sample S-1) showed the highest average j_{corr} of 17.0 nA cm^{-2}. However, when 30%N_2 was introduced into the plasma, the mixed 70%Ar + 30%N_2 plasma-assisted surface modified bare media without COC (sample S-2) showed reduction in j_{corr} to 11.4 nA cm^{-2}. Nevertheless, when 50%N_2 was introduced into the plasma, the mixed 50%Ar + 50%N_2 plasma-assisted surface modified bare media without COC (sample S-3) showed j_{corr} of 15.5 nA cm^{-2}, which, although lower than sample S-1, was higher than sample S-2. Thus, the electrochemical corrosion results for plasma treated bare media without COCs indicated that the inclusion of nitrogen in Ar plasma has an advantageous effect in reducing the corrosion propensity of the media, mainly at the plasma composition of 70%Ar + 30%N_2. For the plasma-assisted surface modified media with COCs, sample S-4, which has the combination of 100%Ar plasma-assisted surface modified media with ~1.5 nm COC, showed an average j_{corr} of 3.5 nA cm^{-2}. However, the average j_{corr} was reduced to 2.9 nA cm^{-2} in both samples S-5 and S-6, which have the combinations of 70%Ar + 30%N_2 plasma-assisted surface modified media with ~1.5 nm COC and 50%Ar + 50%N_2 plasma-assisted surface modified media with ~1.5 nm COC, respectively. This also indicated that compared to sample S-4, samples S-5 and S-6 showed higher corrosion resistance, which may be due to the nitrogen plasma-assisted pre-surface modification of media. However, among samples S-5 and S-6, which were subjected to different plasma modification compositions but had similar COC thickness (~1.5 nm), the corrosion resistance was found to be similar. Furthermore, the j_{corr} of commercial media with commercial COC of thickness 2.7 nm (sample S-7) was also extracted and found to be 2.9 nA cm^{-2}, which was similar to the j_{corr} of samples S-5 and S-6. This demonstrated the effectiveness of nitrogen plasma-assisted pre-surface modification of media in providing adequate corrosion protection of underlying media at lower COC thicknesses of ~1.5 nm in samples S-5 and S-6, which was ~44% thinner with respect to commercial COC in sample S-7. Likewise, to check the consistency of the results, the electrochemical corrosion measurements were repeated on four to five locations per sample as well as on more than one sample. The results were found to be almost similar.

The concept of protection efficiency (PE) was also used to compare the corrosion protection among different samples. In order to measure the PE, sample S-1 was used as the reference. The corrosion PE was calculated using the formula:

$$\%PE = \frac{j^0_{corr} - j_{corr}}{j_{corr}} \times 100$$

where j^0_{corr} is the value of the extrapolated corrosion current density of bare magnetic media sample S-1. The calculated PEs of different

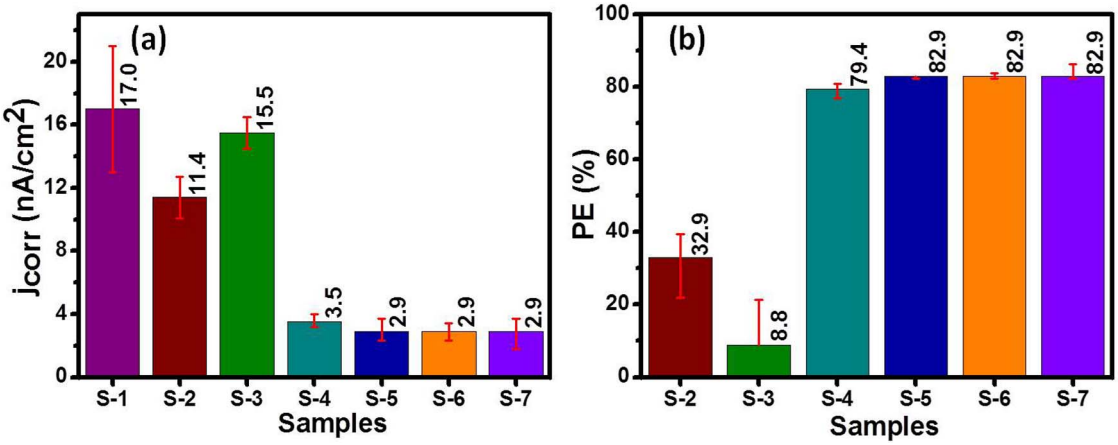

Figure 3 | **Electrochemical corrosion analysis.** Variations of (a) corrosion current density (j_{corr}) and (b) protective efficiency (PE) for different samples.

samples were plotted in Figure 3b. Based on the results shown in Figures 3a and 3b and taking the tribological results into consideration, sample S-2 was found to be the best among plasma-assisted surface modified media without COCs; sample S-5 was found to be the best among plasma-assisted surface modified media with COCs; and overall, sample S-5 was found to be the best among all the samples studied in this work. Hence, the combination of 70%Ar + 30%N_2 plasma-assisted surface modification of media with ~1.5 nm COC provided the best protection to the underlying media without any compromise to its magnetic properties (*see supplementary information S6*).

Surface energy measurements were performed on samples S-4 to S-7 by two types of liquids: one with only a dispersive component, i.e. diiodomethane and the other with both dispersive and polar components, i.e. water (*see supplementary information S7*). The results indicated that samples S-5 and S-6 showed considerably lower surface polarity than sample S-4. This suggested that the introduction of nitrogen in Ar plasma (mixed Ar + N_2 plasma) for the surface modification of media is advantageous in terms of reducing the surface polarity of the media with COC. Among all the samples, the lowest surface polarity was observed in sample S-5. On the other hand, commercial media sample S-7 showed higher surface polarity. The low surface polarity could be beneficial for reducing corrosion and oxidation at lower COC thicknesses (<2 nm).

Structural analysis. UV and visible Raman spectroscopy measurements were performed to probe the microstructures of carbon on the carbon overcoated samples. The Raman spectra of plasma-assisted surface modified media without COCs were also recorded to determine the background and confirm that the carbon peak observed in the carbon-containing samples is due to deliberately grown carbon. Figures 4a–4e show the UV Raman spectra and Figures 4f–4j show the visible Raman spectra of the plasma-assisted surface modified media samples with and without COCs (which correspond to samples S-1, S-2, S-4, S-5 and S-6 respectively). In both the UV and visible Raman spectra, samples S-1 and S-2, which were surface modified media without COCs, showed no signal related to carbon in the range of 1100–1800 cm^{-1}. On the other hand, samples S-4, S-5 and S-6 gave a strong signal in the Raman spectra corresponding to amorphous carbon, representing its characteristic D and G peaks. These results suggest that the carbon signal which appeared in samples S-4, S-5 and S-6 corresponded to the presence of the COC grown by PDC sputtering. Since UV Raman spectroscopy can give more accurate information about sp^3 carbon bonding, we first discuss the UV Raman spectra for samples S-4 to S-6. In order to investigate the differences in the microstructure of COCs used in different surface modified media samples, the UV Raman spectra of samples S-4, S-5 and S-6 were plotted together on the same graph after baseline correction, as shown in Figure 4b. As can be seen, the UV Raman spectra of all these COCs were found to be almost similar, indicating that the variation in the gaseous compositions of the plasma from 100%Ar to the other two Ar + N_2 mixtures during surface modification of media before deposition of COC did not have any significant impact on the microstructure of the COCs. To obtain the exact D and G peak positions and intensity ratio of the D peak to G peak (I_D/I_G), the UV Raman spectra of the COCs in the three overcoated samples were fitted with two Lorentzian components, as shown in Figures 4c–4e. In the Raman spectra of the amorphous carbon films, the D peak arises due to the breathing mode of sp^2 carbon atoms in aromatic rings, whereas the G peak arises from the in-plane bond stretching motion of all pairs of sp^2 carbon atoms in both the aromatic rings and aliphatic chains of carbon. The G peak position is an important parameter to understand the microstructure of amorphous carbon films in terms of sp^3 and sp^2 carbon bonding, whereas the I_D/I_G ratio provides information about ring-like sp^2 cluster formation[12,30–32]. The value of the G peak position arising from the pulsed DC deposition of COCs in these samples was calculated to be 1586 ± 1 cm^{-1} whereas the I_D/I_G ratio was estimated to be 0.85 ± 0.01. These results indicated that the microstructures of the COCs used in samples S-4, S-5 and S-6 were almost all similar in terms of sp^3 carbon bonding.

On the other hand, visible Raman spectroscopy is mainly sensitive to sp^2 carbon bonding and clustering. We have also analyzed the visible Raman spectra of COCs in samples S-4 to S-6 to probe the pre-surface modification induced changes in sp^2 bonding and ring-like sp^2 clustering of COCs. The visible Raman spectra of samples S-4, S-5 and S-6 were plotted together on the same graph after baseline correction, as shown in Figure 4g. In contrast to the UV Raman spectra, the visible Raman spectra of all these COCs were not similar in terms of the intensity of the D and G peaks and could have some change in the G peak position as well. Hence, to obtain the exact D and G peak positions and I_D/I_G ratio, the visible Raman spectra of the COCs in samples S-4 to S-6 were fitted with two Lorentzian components, as shown in Figures 4h–4j. The visible Raman spectra of all the COCs revealed the presence of the characteristic D and G peaks of amorphous carbon. The G peak positions in samples S-4, S-5 and S-6 were observed to be at 1571 cm^{-1}, 1560 cm^{-1} and 1569 cm^{-1}, respectively, and their I_D/I_G ratios were found to be 1.0, 0.7 and 1.0, respectively. The results indicated that the COC in sample S-5 possessed slightly less ring-like sp^2 clusters than the other two samples. Moreover, the difference in the G peak positions seen in sample S-5 when compared with samples S-4 and S-6 (which have almost similar G peak positions) could be due to the change in sp^2 induced

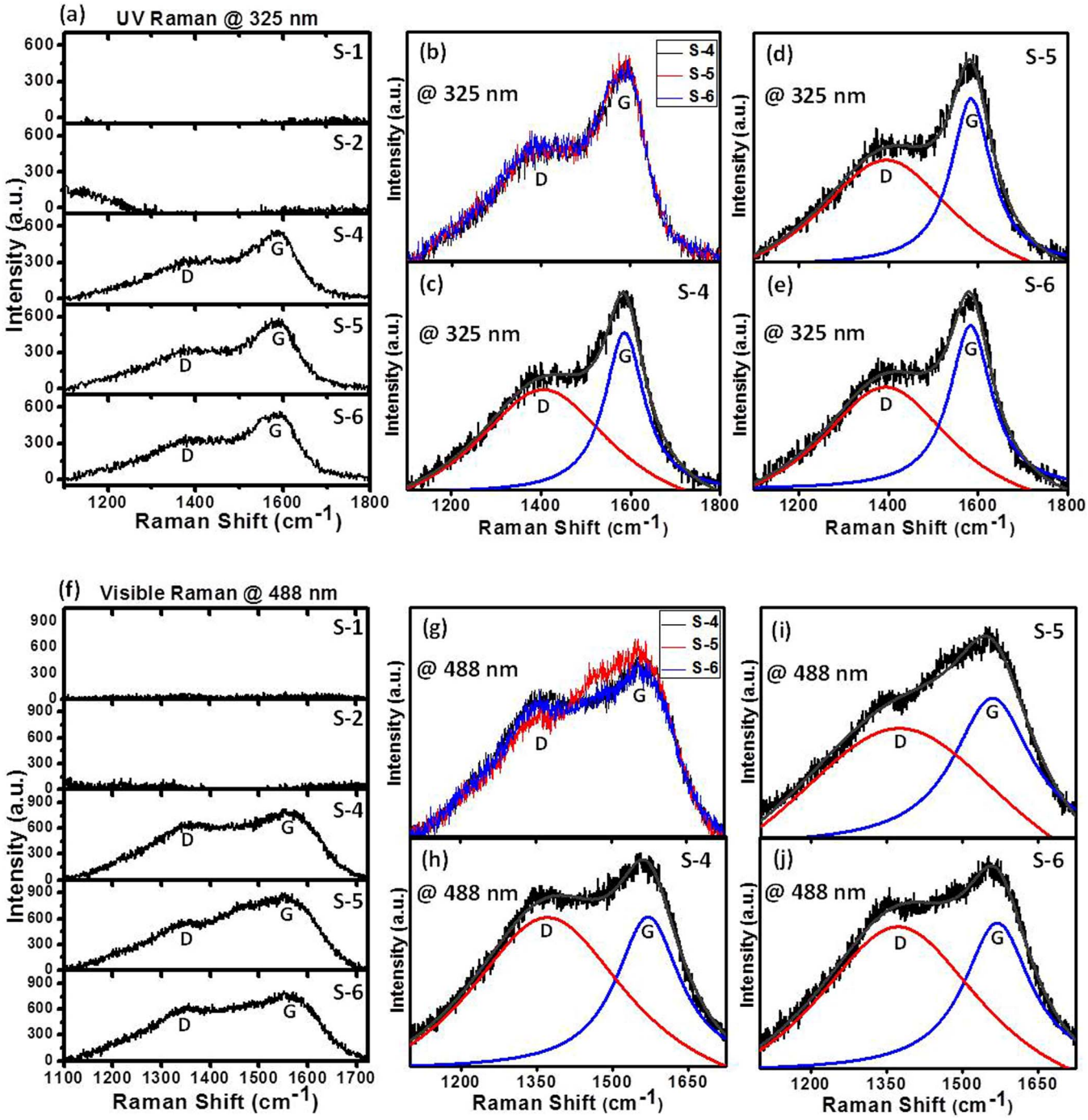

Figure 4 | UV (325 nm) and Visible (488 nm) Raman analyses of the prepared samples. (a)–(e) UV Raman spectra of samples S-1, S-2, S-4, S-5 and S-6 without and with fittings, (f)–(j) visible Raman spectra of samples S-1, S-2, S-4, S-5 and S-6 without and with fittings. The fitting was performed using two Lorentzian components corresponding to the D and G peaks.

ordering, negating any role of sp^3 carbon bonding as confirmed by the similar G peak position found in the UV Raman spectra of all COCs. Thus, the UV and visible analyses indicated that the COCs in samples S-4, S-5 and S-6 could have similar sp^3 carbon bonding but slight differences in the sp^2 carbon ordering.

Carbon hybridization, interfacial bonding and oxidation analysis. XPS measurements were performed to investigate the chemical structure of COCs and the oxidation condition of underlying media for different samples. Figures 5a–5c show the deconvoluted C 1s core level spectra of samples S-4, S-5 and S-6, after background subtraction in Shirley mode. The deconvolution of the C 1s core level spectrum in each sample was performed with four Gaussian curves, which correspond to the sp^2 carbon bonding (sp^2C), sp^3 carbon bonding (sp^3C), C–O bonding and C=O bonding[12,14,18,20,33,34] (*see supplementary information S8.1*). Since sp^3C bonding is the key property of COCs in achieving excellent toughness, wear resistance and film coverage to effectively protect the underlying media[12,16–20], hence, we mainly concentrate on estimating the sp^3C bonding fractions by an area ratio method for all the ultrathin COCs. A comparison of the sp^3C fractions of COCs for samples S-4, S-5 and S-6 is shown in Figure 5d. The sp^3C bonding fractions of the COCs in all the samples were generally similar and were found to be in the range of ~20.5 to 22.5%. Hence, the XPS results corroborated with

the results obtained from Raman analysis, indicating that the gaseous composition of the plasma used during surface modification of media in the three cases has no effect on the sp^3C bonding of the COCs.

After analyzing the C 1s core level spectra, the Co $2p_{3/2}$, O 1s and N 1s core level spectra were also studied. Figures 6a–6c show the N 1s core level spectra of samples S-2, S-5 and S-6. All these spectra indicated the presence of nitrogen at the media surface as a consequence of using an Ar + N_2 plasma during media surface modification. The most interesting and important aspect here is to investigate the role of the gaseous composition of mixed Ar + N_2 plasma in improving the underlying media's surface properties (which is mainly made up of Co). Figures 6d–6h show the Co $2p_{3/2}$ core level spectra of samples S-1, S-2, S-4, S-5 and S-6, respectively. It is evident from Figure 6d that sample S-1 showed a very small peak (labelled #1) at ~778.1 eV, and a very broad and intense peak (labelled #2) at ~780.3 eV. Peak #1 corresponds to metallic Co, while peak #2 is allotted to oxidized Co. Peak #2 is dominant over peak #1, indicating that bare magnetic media, even after surface modification using 100%Ar plasma, is mostly oxidized, at least at the upper surface of the media. Surprisingly, when the gas composition of the plasma was changed to 70%Ar + 30%N_2 (Sample S-2), peak #1 in the Co $2p_{3/2}$ core level spectrum in Figure 6e was increased and simultaneously affected the intensity of peak #2. This suggests that the inclusion of 30%N_2 in mixed Ar + N_2 plasma enhances the metallic bonding fraction of Co after surface modification. Interestingly, when the COCs were applied onto the surface modified media samples, the Co $2p_{3/2}$ core level spectra of samples S-4, S-5 and S-6 showed an intense peak #1 with a very weak and broad peak #2. This suggested that the application of a COC increases (reduces) the metallic (oxide) content of Co, and hence provides improved oxidation resistance to underlying media. The O 1s spectra of samples S-1, S-2, S-4, S-5 and S-6 were also recorded and presented in Figure 6i to detect the amount of oxygen present on the modified media surface/interface with and without COCs. It is evident from the spectra that the O 1s peak intensity was the highest in sample S-1, whereas the peak intensity was significantly reduced in sample S-2. This leads us to the same conclusion that having 30%N_2 during plasma-assisted surface modification of media helps in enhancing the oxidation resistance of the media. The intensity of the O 1s peak was much lower in samples S-4, S-5 and S-6 due to the presence of COCs contributing to oxidation protection.

Further investigation into the oxidative and metallic states of Co as well as its other bonding environments within these samples was carried out. The Co $2p_{3/2}$ core level spectra were deconvoluted with various Lorentzian-Gaussian components after executing Shirley background subtraction. Figures 7a–7e show the deconvoluted Co $2p_{3/2}$ core level spectra of samples S-1, S-2, S-4, S-5 and S-6, respectively. Samples S-1 and S-4 each showed four peaks, while samples S-2, S-5 and S-6 each showed five peaks. The first four peaks in all the samples corresponded to Co (metallic), Co (oxide such as Co_2O_3), Co (oxide/hydroxide such as Co-O, Co_3O_4, CoOOH) and Co (oxide/hydroxide such as Co-O, Co_3O_4, $Co(OH)_2$), respectively[35–41]. An additional fifth peak was found in samples S-2, S-5 and S-6 corresponding to Co-N_x bonding[42–44], due to interaction of nitrogen from the mixed Ar + N_2 plasma with Co during surface modification. (*See*

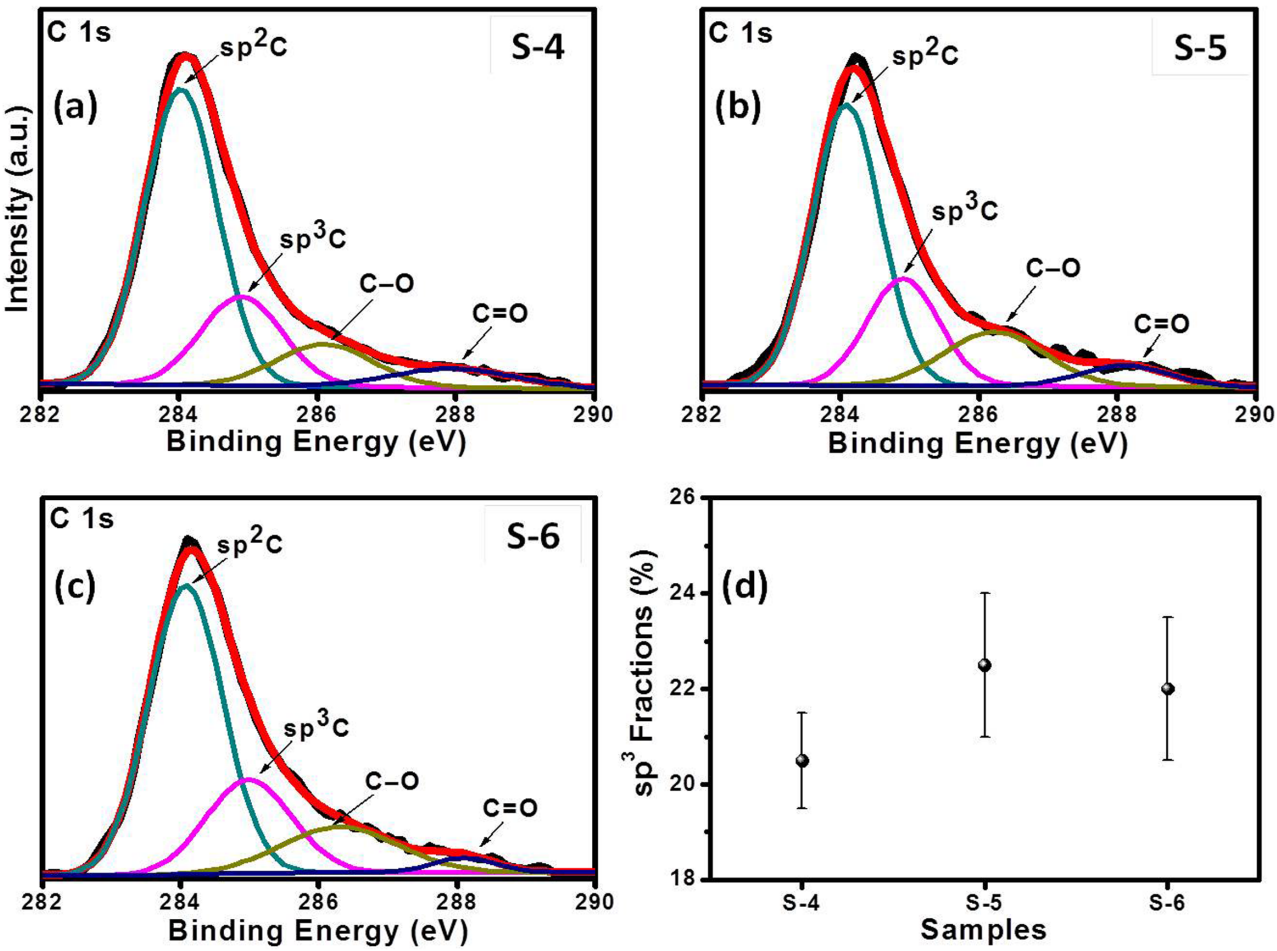

Figure 5 | Carbon hybridization analysis by XPS. Deconvolution of the C 1s core level spectra for samples (a) S-4, (b) S-5 and (c) S-6. (d) Variation of sp^3 fractions for different samples.

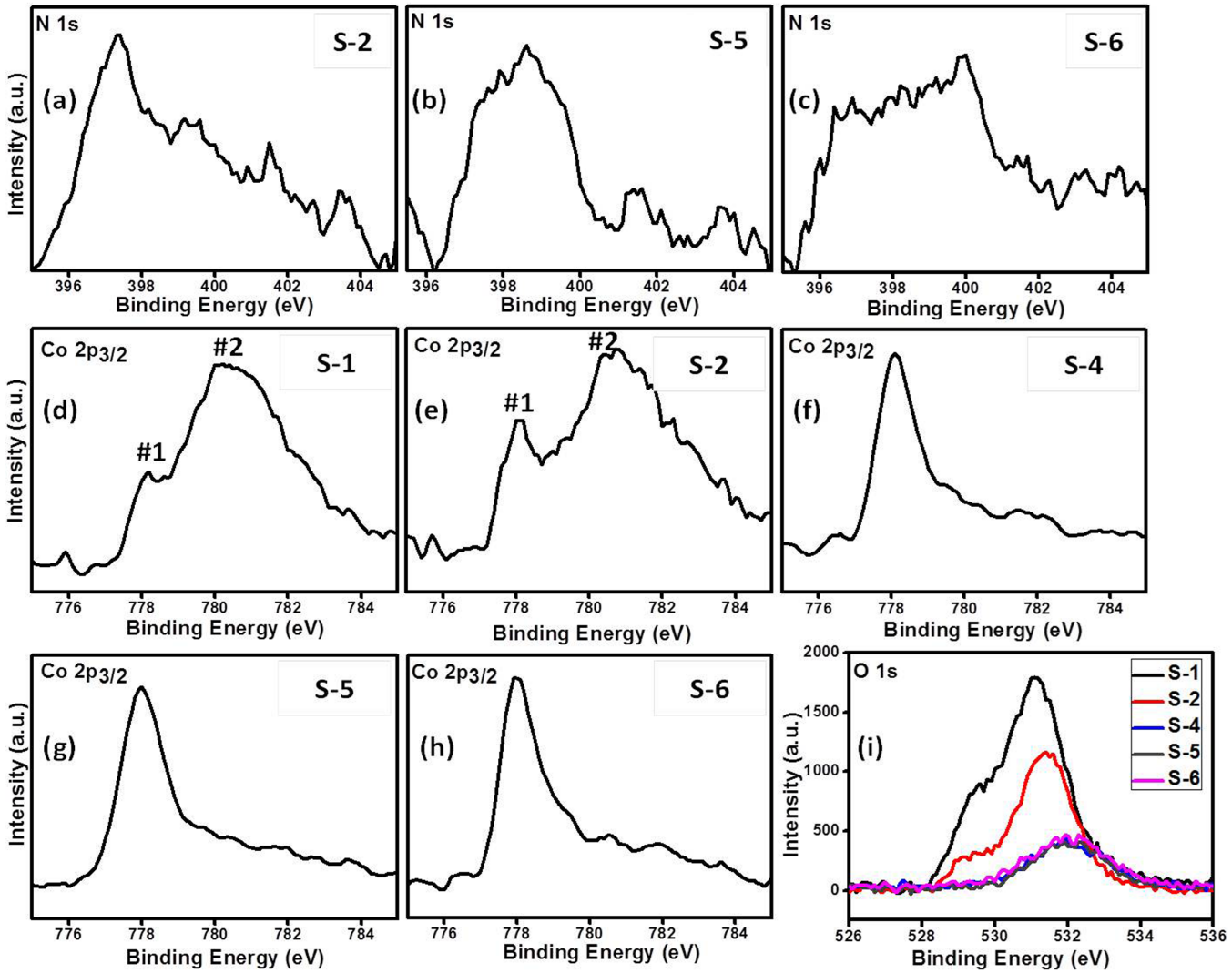

Figure 6 | Various XPS core level spectra for the analyses of oxidation and interfacial bonding. (a)–(c) N 1s core level spectra of samples S-2, S-5 and S-6, respectively, (d)–(h) Co $2p_{3/2}$ core level spectra of samples S-1, S-2, S-4, S-5 and S-6, respectively, and (i) O 1s core level spectra of different samples.

supplementary information S8.2 for a table summarizing the peak positions of various bonding states of cobalt). Given that reducing the oxidation of media from ambient is essentially required to enhance the durability of HDDs, the content of the metallic and oxide states of Co was determined using an area ratio method and given in Table *S8.2.2* (*see supplementary information S8*). The role of nitrogen in reducing the oxide content of Co is revealed by comparing samples S-1 and S-2 for the case of media without COCs, and samples S-4, S-5 and S-6 for the case of media with COCs. After media surface modification, the introduction of 30%N_2 in mixed Ar + N_2 plasma helped to increase the metallic bonding fraction of Co (~24% in sample S-2) as compared with 100%Ar plasma in sample S-1, which gave a metallic Co bonding fraction of ~14%. Similarly, after COC deposition onto the surface modified media, the metallic Co fraction in samples S-4, S-5 and S-6 was observed to be 60.3%, 72.0% and 68.0% respectively. Even with commercial media with thicker conventional COC as in sample S-7, it showed a metallic Co fraction of ~68%. Thus, the results indicated the effectiveness of using the 70%Ar + 30%N_2 gaseous composition during plasma-assisted surface modification of media with COC providing maximum protection for the media from oxidation.

Furthermore, the N 1s core level spectra were deconvoluted to probe the various bonding configurations of nitrogen with media and COCs. N 1s core level spectra were deconvoluted with various Lorentzian-Gaussian components after performing Shirley background subtraction. Figures 7f–7h display the deconvoluted N 1s core level spectra of samples S-2, S-5 and S-6, respectively. Sample S-2 (without COC) showed four peaks, while samples S-5 and S-6 (with COCs) each showed five peaks. The four peaks, namely N1, N2, N3 and N4, were found to be common in samples S-2, S-5 and S-6, which corresponded to Co-N_x & Cr_2-N bonding, metal-N-pyridyl-like bonding, graphitic C=N bonding, and N-O bonding, respectively[42,43,45–48]. Since sample S-2 did not have COC, the presence of graphitic C=N bonding in sample S-2 may be attributed to the reaction of nitrogen with surface carbon contamination. An additional fifth peak "N5" was observed only in the samples with COCs (samples S-5 and S-6). This peak N5 corresponded to nitrogen bonded in the pyridine-like structure[47–49]. See *supplementary information S8.4* for a table summarizing the peak positions of various bonding states of nitrogen with metals, carbon and oxygen.

Discussion

The results from the ball-on-disk tribological tests, electrochemical corrosion tests, and oxidation analyses by XPS for both surface modified and reference media samples suggest that the incorporation of nitrogen gas, particularly when a gaseous composition of 70%Ar + 30%N_2 is used in an Ar + N_2 mixture during plasma-assisted surface modification of media, has advantageous effects in lowering and

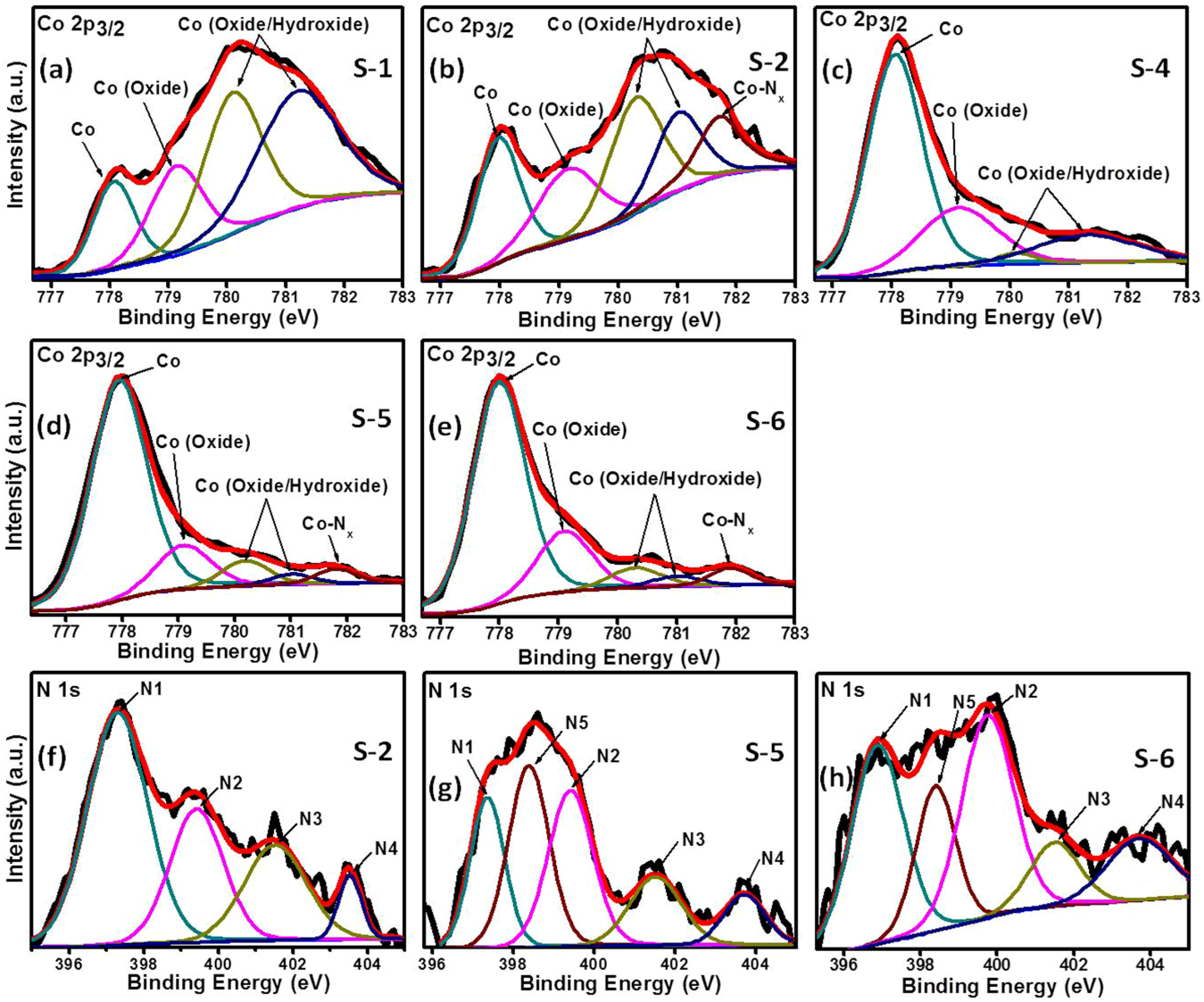

Figure 7 | Evaluation of interfacial bonding and quantitative analysis of oxidation protection of the media layer. Deconvolution of the core level spectra of (a)–(e) Co $2p_{3/2}$ and (f)–(h) N 1s for different samples.

stabilizing friction, improving wear resistance, enhancing corrosion resistance, and reducing oxidation resistance of the media in both cases with and without COCs, without affecting the magnetic properties of the media. Moreover, surface energy measurements suggest that when the surface modification is performed using 70%Ar + 30%N_2 and then coated with 1.5 nm COC, the surface polarity of the prepared sample (S-5) is seen to be significantly lower. However, the UV and visible Raman spectroscopy and C 1s XPS results revealed that using different gaseous compositions of either 100%Ar or mixed Ar + N_2 had no significant influence on modifying the microstructures of the pulsed DC sputter-deposited COCs in terms of sp^3C bonding. However, since visible Raman is predominantly sensitive to sp^2 bonding and sp^2 clustering, sample S-5 showed slightly less ring-like sp^2 cluster formation than samples S-4 and S-6, as indicated by the I_D/I_G ratio. Overall, the microstructures of the COCs in samples S-4, S-5 and S-6 can be assumed to be similar. It is therefore pertinent for us to understand how the inclusion of N_2, mainly with a composition of 70%Ar + 30%N_2 during the plasma-assisted surface modification process, improves the surface properties of the media in terms of better protection, despite having similar COC microstructures (and properties).

Interfaces and interfacial bonding play a very crucial role in influencing the friction and wear resistance of overcoat materials. In our case, unlike 100%Ar plasma treated media surfaces with COCs, the presence of nitrogen in mixed Ar + N_2 plasma for surface modified media with COCs helped in the formation of a graded interfacial layer between the media and the COC. This can be confirmed by analyzing the XPS Co $2p_{3/2}$ and N 1s core level spectra of samples S-5 and S-6. As compared to sample S-4, where surface modification was performed using 100%Ar plasma, samples S-5 and S-6 showed additional Co-N_x, Cr_2-N, metal-N-pyridyl, pyridine-like, and graphitic C=N bonding (Figures 7d, 7e, 7g, 7h). Even for surface modified media without COCs, we found that when the media was modified using 70%Ar + 30%N_2 plasma (sample S-2), it showed additional Co-N_x, Cr_2-N, metal-N-pyridyl, and graphitic C=N bonding (Figures 7a, 7b, and 7f) as compared to the media modified using 100%Ar plasma (sample S-1). It should be noted that nitrogen plasma-assisted treatments of conventional engineering materials such as steel have also been found to develop a graded surface/interface before deposition of a protective overcoat. The development of a graded interface can reduce the interfacial free energy, leading to an increase in the amount of work required for delamination[50]. Similarly, in our case, the formation of a graded layer in samples S-5 and S-6, as compared with sample S-4, could reduce the interfacial free energy. Moreover, increased interfacial bonding between nitrogen, media and COC can improve the interfacial strength and adhe-

sion of COCs with media. Consequently, the media modified using mixed Ar + N_2 plasma and possessing 1.5 nm COC (samples S-5 and S-6) showed lower friction and higher wear resistance than the media modified using 100%Ar plasma with 1.5 nm COC (sample S-4). However, between samples S-5 and S-6, slightly better tribological performance in terms of stable friction and higher wear resistance was observed in sample S-5. One possible reason for this is that from XPS analysis, we found that the bonding fraction corresponding to nitrogen bonded in a pyridine-like structure was higher in sample S-5 than sample S-6. Since the increase in the nitrogen derived pyridine-like structure in the sp^2 and sp^3 bonded network assists to improve the toughness of the carbon films[48,49], we hypothesized that the relatively higher amount of pyridine-like bonding observed at the surface modified media and COC interface in sample S-5 would lead to its higher toughness and hence, stable friction and higher wear resistance compared to sample S-6. Further, while investigating the properties of nitrogen incorporated carbon films, Wei *et al.*[51] demonstrated that the wear durability initially increases with an increasing amount of nitrogen percentage from 0% to 30%, beyond which the wear durability deteriorates with further increase in the nitrogen percentage up to 50%. This suggested that the nitrogen percentage of 30% could be an optimum for Wei *et al.*[51] as well as in our case, though the structural designs of the coatings are different. Moreover, mixed Ar + N_2 plasma treated media without COC, mainly at the gaseous composition of 70%Ar + 30%N_2 for plasma treatment (sample S-2), showed significantly lower friction and higher wear resistance than the media treated with 100%Ar plasma (sample S-4). This is attributed to the formation of several nitrogen originated bonding at the media surface. Overall, a mixed 70%Ar + 30%N_2 plasma used for surface modification of media before COC deposition is found to be optimal, and provides good surface properties and enhanced interfacial bonding between the media and the overcoat by forming nitrogen-based bonds with Co and Cr in the media, and C in the COC. This, in turn, helps to improve the wear resistance and tribological performance of the COC.

A second important role of nitrogen in plasma-assisted surface modification of the media is seen to be that of efficiently removing the ambient oxygen or native oxides formed on the surface of the media. We found that when compared with 100%Ar plasma, the introduction of nitrogen in the mixed 70%Ar + 30%N_2 plasma efficiently removed the ambient oxygen from the media surfaces. As a consequence of that, the content of Co-metallic (Co-oxide) was found to be higher (lower) in sample S-2 than S-1 for surface modified media without COCs, and it was observed to be higher in sample S-5 than S-4 for surface modified media with COCs (*see supplementary information S8.2*). Even sample S-6, which was subjected to 50%Ar + 50%N_2 plasma-assisted surface modification and held 1.5 COC, showed higher (lower) Co-metallic (C-oxide) content than sample S-4. The efficient removal of oxygen due to the presence of nitrogen in plasma was also indicated by the analysis of the O 1s spectra (Figure 6i) because for surface modified media without COCs, the intensity of the O 1s peak was comparatively lower in sample S-2 than sample S-1. The schematic view for the comparison of 100%Ar and mixed Ar + N_2 (mainly 70%Ar + 30%N_2) plasma-assisted removal of oxygen from media surfaces before the deposition of COCs, and the reaction of nitrogen with media to form nitrogen derived interfacial bonding and graded layer, are illustrated in Figure 8. The removal of a high amount of ambient oxygen from the media surface would lead to better adhesion between the COC and media. Moreover, removal of oxygen and addition of nitrogen at the media surface could improve the wear resistance arising from surface passivation by nitrogen. As a result, reduction of friction and improvement of wear resistance were observed in sample S-2 as compared to sample S-1 for surface modified media without COCs, and these properties were better in sample S-5 than sample S-4 for surface modified media with COCs. Thus, the sample sequence in terms of the extent of oxidation protection for media with COCs is as follows: S-5 > S-6 > S-4, leading to tribological performance in the same sequence. The efficient removal of oxygen from the media surface due to inclusion of nitrogen in the plasma has also lowered the surface polarity in samples S-5 and S-6, compared to sample S-4. Moreover, corrosion resistance was also found to be better in samples S-5 and S-6 than sample S-4, which may be due to the reduction of surface oxygen and generation of nitrogen-based interfacial bonding. Amongst samples S-5 and S-6, which were Ar + N_2 plasma-modified media using different gaseous compositions with COCs, slightly lower surface polarity but comparable corrosion resistance was observed in sample S-5 compared to sample S-6. It is interesting to note that mixed Ar + N_2 plasma-modified media with 1.5 nm COCs showed comparable/better tribological, oxidation and corrosion resistance and surface properties than 2.7 nm thicker conventional COCs in commercial media (sample S-7). The better tribological properties found in sample S-5 than sample S-7 might be due to combined effects of nitrogen derived enhanced interfacial bonding and lower roughness. Furthermore, Bazzoni *et al.*[52] have investigated the surface hardness of pure CoCrMo-alloys and plasma nitrided CoCrMo-alloys, and found higher hardness and 10 times greater wear resistance in the plasma nitrided CoCrMo-alloy. Hence, we also speculate that plasma-assisted surface modification of media using a gaseous composition of 70%Ar + 30%N_2 could help in surface hardening and hence, improved wear resistance of the media due to the presence of nitrogen.

In summary, an in-situ plasma-assisted surface modification of the media using a gaseous mixture of Ar + N_2 prior to the deposition of COCs is proposed as a novel approach to improve the protection capability of ultrathin sputtered COCs of thickness <2 nm on media. The plasma-assisted surface modifications were performed using three gaseous compositions of 100%Ar, 70%Ar + 30%N_2 and 50%Ar + 50%N_2. By examining the surface roughness, tribological properties, corrosion and oxidation properties, microstructure evolution and surface/interfacial bonding, the following conclusions have been drawn:

1) For the case of surface modified media without any COC, the surface modification process performed in plasma generated with a gaseous mixture of 70%Ar + 30%N_2 was found to show the lowest COF, highest wear resistance, and highest oxidation and corrosion resistance among the other samples.
2) For the case of surface modified media with 1.5 nm COCs grown on top by pulsed DC sputtering, the surface modification process performed in 70%Ar + 30%N_2 plasma was also found to show a lower and stable COF, highest wear resistance, highest oxidation resistance, lowest surface polarity, and comparable corrosion performance among the other samples.
3) The examination of the XPS, UV and visible Raman spectroscopic results revealed that surface modification of the media using the three different gaseous compositions had no influence on the microstructures of the COCs in terms of sp^3C bonding, but visible Raman analysis indicated that sample S-5 could have relatively lower sp^2 clustering.
4) The improved protection of the media owing to the plasma-assisted surface modification process at a gaseous composition of 70%Ar + 30%N_2 can be attributed to the formation of nitrogen-based interfacial bonding and more effective removal of ambient oxygen from the surface of the media by nitrogen, leading to reduced oxidation at the surface/interface and enhanced adhesion of the COCs with the media.
5) Overall, 70%Ar + 30%N_2 plasma modification assisted to improve the protection characteristics of COCs without degrading the magnetic properties of media due to: 1) Increased nitrogen-based interfacial bonding and 2) Sufficient removal of oxygen with minimal removal of the magnetic layer. Hence, for this study, the gaseous composition

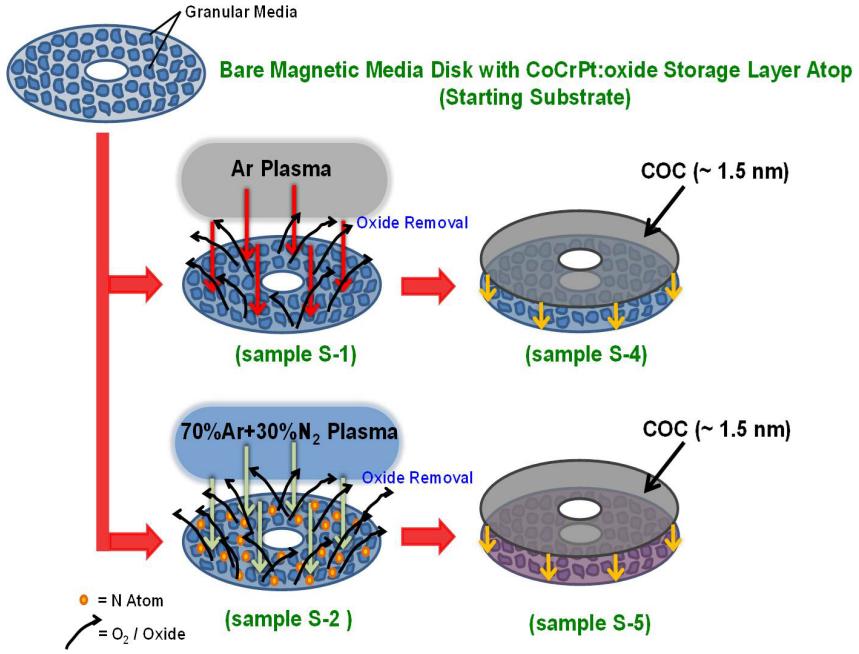

Figure 8 | Schematic illustration of how the mixed Ar + N_2 plasma (mainly 70%Ar + 30%N_2) leads to the formation of nitrogen-based interfacial bonding between media and COC, and how the mixed Ar + N_2 plasma efficiently removes the oxygen as compared to 100%Ar plasma. (a) Granular media with CoCrPt:Oxide storage layer atop, (b) 100%Ar plasma-assisted surface treatment of media followed by (c) COC deposition, (d) 70%Ar + 30%N_2 plasma-assisted surface treatment of media followed by (e) COC deposition. The 70%Ar + 30%N_2 plasma helps to form additional nitrogen-based interfacial bonding and efficiently removes the oxygen from media as compared to surface treatment using 100%Ar plasma. Thus, 70%Ar + 30%N_2 plasma was found to be advantageous in terms of improving interfacial strength by creating additional interfacial bonding, leading to high wear resistance and stable and low friction, in addition to better corrosion/oxidation protection and low surface polarity.

of 70%Ar + 30%N_2 is the optimum for plasma-assisted surface treatment of the media.

These findings are significant due to three reasons: 1) Good protection to the media can be realized at a low thickness of ~1.5 nm, which is desirable for future hard disk drives with high areal densities; 2) Employing a gaseous composition of 70%Ar + 30%N_2 in plasma-assisted pre-surface modification of the media can lead to improved protective characteristics of sputtered COCs, even at the COC thickness of <2 nm; and 3) Using this approach, both the surface modification process and COC deposition can be performed in-situ using a facile process of magnetron sputtering.

Methods

Sample preparation. Specially prepared commercial 2.5″ CoCrPt:oxide-based hard disk media without commercial COC and without a lubricant layer, provided by our industrial collaborators, were used as starting substrates. The surface modifications of the media by plasma as well as the COC depositions on the plasma modified media were performed in-situ within a standard computer-controlled magnetron sputtering system (AJA International) housed in a class 10 K cleanroom. The cylindrical sputtering chamber has a diameter of ~34.8 cm, which was evacuated to achieve a base pressure of $\sim 2 \times 10^{-8}$ Torr, and the substrate-to-target distance was maintained at ~15.0 cm throughout the surface modification and deposition processes. Plasma-assisted surface modifications of the media were carried out using a substrate RF bias power of 40 W, while maintaining a working pressure of 1.0×10^{-2} Torr and a total gas flow rate of 20 sccm. The surface modification time was kept constant at 3 minutes for all the samples. Subsequently, ultrathin COC depositions on the surface modified media were carried out using a pulsed DC sputtered deposition scheme in 100%Ar atmosphere, using 100 W of power supplied to a 99.999% pure graphite target with pulsed frequency of 150 kHz and a pulse duration of 2.6 μs. A working pressure of 3.0×10^{-3} Torr and Ar gas flow rate of 20 sccm were maintained throughout the deposition. Only the Ar and N_2 gaseous compositions used to generate the plasmas during surface modification were varied as follows: 100%Ar, 70%Ar + 30%N_2, and 50%Ar + 50%N_2.

A total of six samples were prepared, of which three were plasma-assisted surface modified media without COCs (labeled S-1 to S-3), and the other three were plasma-assisted surface modified media with COCs (labeled S-4 to S-6). The performance of these samples was also compared to a reference commercial media sample containing its original commercial COC (~2.7 nm thickness) but without its lubricant layer (labeled S-7). A table summarizing the description and nomenclature of samples used in this work is given in *supplementary information S1*.

Characterizations. High resolution transmission electron microscopy (HRTEM, Philips FEG CM300) in cross-section geometry was used to measure the thicknesses of the COCs. Samples S-4 to S-7 were prepared for cross-section HRTEM imaging by first sputter depositing a titanium nitride (TiN) or tantalum (Ta) capping layer on top of the COCs. Next, the samples were diced into smaller pieces and then the surfaces were attached together using an epoxy adhesive. Due to the similar contrast between carbon and epoxy, the TiN or Ta capping layer provided a clear distinction between the COC and the epoxy adhesive during imaging. Finally, the samples were thinned down by mechanical polishing and ion milling to a thickness suitable for HRTEM imaging.

The surface roughness of all the samples were measured using tapping mode atomic force microscopy (AFM, Bruker Innova) equipped with a silicon cantilever and tip of radius ~8 nm. The roughness measurements were performed across a scan area of 2 μm × 2 μm at three different locations on each sample surface, from which a mean value was taken.

Ball-on-disk tribological tests were carried out on all the samples using a nano-tribometer (CSM Instruments) to examine the friction and wear resistance of surface modified media with and without COCs. The tests were conducted in a clean room environment (temperature of 23 ± 1°C and relative humidity of 55 ± 5%) using a sapphire ball with diameter of 2.0 ± 0.1 mm and surface roughness of 5.0 ± 0.1 nm as the counterface material. During the ball-on-disk tests, a normal load of 20 mN and a rotational speed of 100 rpm (linear speed = 2.1 cm/s) for 10,000 cycles were kept constant for all the samples. After the tests, the wear track and ball images for each sample were captured using an optical microscope.

The adequate protection of the hard disk media from corrosion or oxidation is critical when the thickness of sputtered COC decreases to <2–3 nm. The corrosion leads to the deterioration of the magnetic properties of the media and hence, loss of the recorded information. To understand the role of nitrogen in plasma-assisted surface modification of media in preventing the corrosion of media with and without ultrathin COCs (<2 nm), a custom-made three-electrode electrochemical corrosion system was used to take potentiodynamic polarization measurements on these samples. An electrolyte solution of 0.1 M NaCl was used during the test, and a sample surface area of 0.24 cm^2 was exposed to the electrolyte. Each electrochemical test consisted of an anodic sweep and a cathodic sweep where the potential was varied and the corresponding current was measured. Every sweep was conducted at a different location on the sample, with at least three sets of tests (6 sweeps) conducted on each sample.

Since the surface modification technique applied in this work is intended only to affect the topmost surface of the media, it is important to understand how the surface

modifications in different plasmas affect the surface and interface properties of the samples. To do this, the chemical bonding within the COC, at the COC-media interface and at the surface of the media, was probed using X-ray photoelectron spectroscopy (XPS, VG ESCALAB 220I-XL). XPS measurements were performed in ultrahigh vacuum (UHV) conditions of $\sim 10^{-9}$ Torr by employing a monochromatic Al-Kα X-ray source (1486.6 eV). In addition, the microstructures of the COCs in these samples were examined with ultra-violet (UV, 325 nm) and visible (488 nm) Raman spectroscopy (Jobin Yvon LABRAM-HR). The 325 nm UV and 488 nm visible excitations were achieved with a He-Cd laser and an Ar laser, respectively, and the spot size was fixed at ~ 1 μm for the analysis. However, to avoid damage of the ultrathin COCs due to the intense laser heating of the sample surface, the laser power was kept low, while other parameters such as the charge coupled device's (CCD) exposure and data acquisition time were synchronized in order to obtain a reasonable signal-to-noise ratio for all samples. The relative intensity ratios of the COCs were compared at various locations of the sample surfaces to distinguish the nature of the carbon bonding with an accuracy of $<2\%$.

1. Marchon, B., Pitchford, T., Hsia, Y.-T. & Gangopadhyay, S. The head-disk interface roadmap to an areal density of 4 Tbit/in^2. *Adv. Tribol.* **2013**, 1–8 (2013).
2. Pan, L. & Bogy, D. B. Data storage: heat assisted magnetic recording. *Nat. Photonics* **3**, 189–190 (2009).
3. Wood, R., Williams, M., Kavcic, A. & Miles, J. The feasibility of magnetic recording at 10 terabits per square inch on conventional media. *IEEE Trans. Magn.* **45**, 917–923 (2009).
4. Piramanayagam, S. N. Perpendicular recording media for hard disk drives. *J. Appl. Phys.* **102**, 011301 (2007).
5. Park, K. S., Park, Y. P. & Park, N. C. Prospect of recording technologies for higher storage performance. *IEEE Trans. Magn.* **47**, 539–545 (2011).
6. Kundu, S. *et al*. Effect of angstrom scale surface roughness on the self-assembly of polystyrene-polydimethylsiloxane block copolymer. *Sci Rep.* **2**, 617 (2012).
7. Cho, N. H. *et al*. Effects of substrate temperature on chemical structures of amorphous carbon. *J. Appl. Phys.* **71**, 2243–2248 (1992).
8. Li, X. & Bhusan, B. Micro/nanomechanical and tribological characterization of ultrathin amorphous carbon coatings. *J. Mater. Res.* **14**, 2328–2337 (1999).
9. Tsai, H. & Bogy, D. B. Characterization of diamond-like carbon films and their application as overcoats on thin film media for magnetic recording. *J. Vac. Sci. Technol. A* **5**, 3287–3311 (1987).
10. Bernhard, P., Ziethen, C., Ohr, R., Hilgers, H. & Schonhense, G. Investigations of the corrosion protection of ultrathin a-C and a-C:N overcoats for magnetic storage devices. *Surf. Coat. Technol.* **180–181**, 621–626 (2004).
11. Ohr, R., Jacoby, B., Gradowski, M. V., Schug, C. & Hilgers, H. Analytical and functional characterization of ultrathin carbon coatings for future magnetic storage devices. *Surf. Coat. Technol.* **174–175**, 1135–1139 (2003).
12. Dwivedi, N. *et al*. Probing the role of an atomically thin SiN_x interlayer on the structure of ultrathin carbon films. *Sci. Rep.* **4**, 5021 (2014).
13. Wang, N. & Komvopoulos, K. Thermal stability of ultrathin amorphous carbon films for energy-assisted magnetic recording. *IEEE Trans. Magn.* **47**, 2277–2282 (2011).
14. Pathem, B. K. *et al*. Carbon overcoat oxidation in heat-assisted magnetic recording. *IEEE Trans. Magn.* **49**, 3721–3724 (2013).
15. Jones, P. M., Ahner, A., Platt, C. L., Tang, H. & Hohlfeld, J. Understanding Disk Carbon Loss Kinetics for Heat Assisted Magnetic Recording. *IEEE Trans. Magn.* **50**, 3300704 (2014).
16. Bhatia, C. S. *et al*. Ultrathin overcoats for the head/disk interface tribology. *J. Tribol.* **120**, 795–799 (1998).
17. Robertson, J. Requirements of ultrathin carbon coatings for magnetic storage technology. *Tribol. Int.* **36**, 405–415 (2003).
18. Goohpattader, P. S. *et al*. Probing the role of C+ ion energy, thickness and graded structure on the functional and microstructural characteristics of ultrathin carbon films (2 nm). *Tribol. Int.* **81**, 73–88 (2015).
19. Ferrari, A. C. Diamond-like carbon for magnetic storage disks. *Surf. Coat. Technol.* **180–181**, 190–206 (2004).
20. Yeo, R. J. *et al*. Bi-level surface modification of hard disk media by carbon using filtered cathodic vacuum arc: Reduced overcoat thickness without reduced corrosion performance. *Diamond Relat. Mater.* **44**, 100–108 (2014).
21. Samad, M. A. *et al*. A novel approach of carbon embedding in magnetic media for future head/disk interface. *IEEE Trans. Magn.* **48**, 1807–1812 (2012).
22. Robertson, J. Ultrathin carbon coatings for magnetic storage technology. *Thin Solid Films* **383**, 81–88 (2001).
23. Yen, B. K. *et al*. Coverage and properties of a-SiN_x hard disk overcoat. *J. Appl. Phys.* **93**, 8704–8706 (2003).
24. Yen, B. K. *et al*. Microstructure and properties of ultrathin amorphous silicon nitride protective coating. *J. Vac. Sci. Technol. A* **21**, 1895–1904 (2003).
25. Rose, F. *et al*. Ultrathin TiSiN overcoat protection layer for magnetic media. *J. Vac. Sci. Technol. A* **29**, 051502 (2011).
26. Rose, F. *et al*. Low surface enrgy and corrosion resistant ultrathin TiSiC disk overcoat. *J. Appl. Phys.* **113**, 213513 (2013).
27. Tamura, Y., Yokoyama, A., Watari, F., Uo, M. & Kawasaki, T. Mechanical properties of surface nitrided titanium for abrasion resistant implant materials. *Mater. Trans.* **43**, 3043–3051 (2002).
28. Zagonel, L. F., Figueroa, C. A., Droppa Jr, R. & Alvarez, F. Influence of the process temperature on the steel microstructure and hardening in pulsed plasma nitriding. *Surf. Coat. Tech.* **201**, 452–457 (2006).
29. Li, D. J., Guruz, M. U., Bhatia, C. S. & Chung, Y. W. Ultrasmooth CN_x overcoats for 1 Tb/in^2 hard disk drive systems. *Appl. Phys. Lett.* **81**, 1113–1115 (2002).
30. Yeo, R. J. *et al*. Enhanced tribological, corrosion, and microstructural properties of an ultrathin (2 nm) silicon nitride/carbon bilayer overcoat for high density magnetic storage. *ACS Appl. Mater. Interfaces* **6**, 9376–9385 (2014).
31. Ferrari, A. C. & Robertson, J. Interpretation of Raman spectra of disordered and amorphous carbon. *Phys. Rev. B* **61**, 14095–14107 (2000).
32. Ferrari, A. C. & Robertson, J. Resonant Raman spectroscopy of disordered, amorphous, and diamond-like carbon. *Phys. Rev. B* **64**, 075414 (2001).
33. Wang, N. & Komvopoulos, K. Incidence angle effect of energetic carbon ions on deposition rate, topography, and structure of ultrathin amorphous carbon films deposited by filtered cathodic vacuum arc. *IEEE Trans. Magn.* **48**, 2020–2227 (2012).
34. Zhang, H. S. & Komvopoulos, K. Surface modification of magnetic recording media by filtered cathodic vacuum arc. *J. Appl. Phys.* **106**, 093504 (2009).
35. Briggs, D. & Seah, M. P. *Practical Surface Analysis by Auger and X-ray Photoelectron Spectroscopy*. [1–674] (John Wiley & Sons, 1983).
36. McIntyre, N. S. & Cook, M. G. X-ray photoelectron studies on some oxides and hydroxides of cobalt, nickel, and copper. *Anal. Chem.* **47**, 2208–2213 (1975).
37. Wagner, C. D., Riggs, W. M., Davis, L. E., Moulder, J. F. & Muilenberg, G. E. *Handbook of X-ray Photoelectron Spectroscopy*. [1–190] (Perkin-Elmer Corporation, 1979).
38. Barr, T. L. An ESCA study of the termination of the passivation of elemental metals. *J. Phys. Chem.* **82**, 1801–1810 (1978).
39. Biesinger, M. C. *et al*. Resolving surface chemical states in XPS analysis of first row transition metals, oxides and hydroxides: Cr, Mn, Fe, Co and Ni. *Appl. Surf. Sci.* **257**, 2717–2730 (2011).
40. Petitto, S. C., Marsh, E. M., Carson, G. A. & Langell, M. A. Cobalt oxide surface chemistry: The interaction of CoO (100), Co_3O_4 (110), and Co_3O_4 (111) with oxygen and water. *J. Mol. Catal. A: Chem.* **281**, 49–58 (2008).
41. Sampanthar, J. T. & Zeng, H. C. Synthesis of $Co^{II}Co^{III}_{2-x}Al_xO_4$-$Al_2O_3$ nanocomposites via decomposition of $Co^{II}_{0.73}Co^{III}_{0.27}(OH)_{2.00}(NO_3)_{0.23}(CO_3)_{0.02}.0.5H_2O$ in a Sol-Gel-Derived γ-Al_2O_3 matrix. *Chem. Mater.* **13**, 4722–4730 (2001).
42. Morozan, A., Jegou, P., Jousselme, B. & Palacin, S. Electrochemical performance of annealed cobalt-benzotriazole/CNTs catalysts towards the oxygen reduction reaction. *Phys. Chem. Chem. Phys.* **13**, 21600–21607 (2011).
43. Arechederra, R. L., Artyushkova, K., Atanassov, P. & Minteer, S. D. Growth of phthalocyanine doped and undoped nanotubes using mild synthesis conditions for developments of novel oxygen reduction catalysts. *ACS Appl. Mater. Interfaces* **2**, 3295–3302 (2010).
44. Li, M. *et al*. Cobal and nitrogen co-embedded onion-like mesoporous carbon vesicles as efficient catalysts for oxygen reduction reaction. *J. Mater. Chem. A* **2**, 11672–11682 (2014).
45. Wang, L., Zhang, L., Bai, L., Han, L. & Dong, S. Nitrogen, cobal-codoped carbon electrocatalyst for oxygen reduction reaction using soy milk and cobalt salts as precursors. *Electrochem. Comm.* **34**, 68–72 (2013).
46. Jiang, T., Wallinder, I. O. & Herting, G. Chemical stability of chromium carbide and chromium nitride powders compared with chromium metal in synthetic biological solutions. *ISRN Corros.* **2012**, 379697 (2012).
47. Rodil, S. E. & Muhl, S. Bonding in amorphous carbon nitride. *Diamond. Relat. Mater.* **13**, 1521–1531 (2004).
48. Schmidt, S., Czigany, Z., Greczynski, G., Jensen, J. & Hultman, L. Influence of inert gases on the reactive high power pulsed magnetron sputtering process of carbon nitride thin films. *J. Vac. Sci. Technol. A* **31**, 011503 (2013).
49. Neidhart, J., Czigany, Z., Burnell, I. F. & Hultman, L. Growth of fullerene-like carbon nitride thin solid films by reactive magnetron sputtering: role of low energy ion irradiation in determining microstructure and mechanical properties. *J. Appl. Phys.* **93**, 1–14 (2003).
50. Silva, W. M., Airoldi, V. J. T. & Chung, Y. W. Surface modification of 6150 steel substrates for the deposition of thick and adherent diamond-like carbon coatings. *Surf. Coat. Technol.* **205**, 3703–3707 (2011).
51. Wei, B., Zhang, B. & Johnson, K. E. Nitrogen induced modifications in microstructure and wear durability of ultrathin amorphous carbon films. *J. Appl. Phys.* **83**, 2491–2499 (1998).
52. Bazzoni, A., Mischler, S. & Espallargas, N. Tribocorrosion of pulsed plasma-nitrided CoCrMo implant alloy. *Tribol. Lett.* **49**, 157–167 (2013).

Acknowledgments

This research is supported by the National Research Foundation, Prime Minister's Office, Singapore under its Competitive Research Programme (CRP Award No. NRF-CRP 4-2008-06). We acknowledge Ms. Huiru Tan and Ms. June Ong from IMRE for their help in TEM and XPS characterizations, respectively.

Author contributions

N.D. and R.J.Y. prepared samples. N.D., R.J.Y., N.S., S.K. and S.T. performed characterizations. N.D., R.J.Y. and C.S.B. analyzed the data. N.D. and C.S.B. wrote the main manuscript text and prepared figures. All authors reviewed the manuscript.

Additional information

Supplementary information accompanies this paper at http://www.nature.com/scientificreports

Competing financial interests: The authors declare no competing financial interests.

How to cite this article: Dwivedi, N. *et al.* Understanding the Role of Nitrogen in Plasma-Assisted Surface Modification of Magnetic Recording Media with and without Ultrathin Carbon Overcoats. *Sci. Rep.* **5**, 7772; DOI:10.1038/srep07772 (2015).